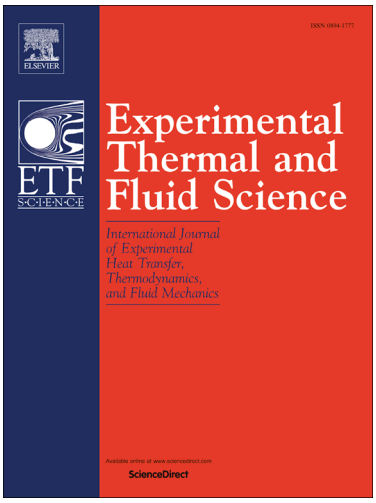

SNS optical fiber sensor for direct detection of phase transitions in C18H38 n-alkane material

Wei Han, Marek Rebow, Xiaokang Lian, Dejun Liu, Gerald Farrell, Qiang Wu, Youqiao Ma, Yuliya Semenova

PII: S0894-1777(18)31873-9
DOI: https://doi.org/10.1016/j.expthermflusci.2019.109854
Article Number: 109854
Reference: ETF 109854

To appear in: *Experimental Thermal and Fluid Science*

Received Date: 30 November 2018
Revised Date: 31 May 2019
Accepted Date: 16 June 2019

Please cite this article as: W. Han, M. Rebow, X. Lian, D. Liu, G. Farrell, Q. Wu, Y. Ma, Y. Semenova, SNS optical fiber sensor for direct detection of phase transitions in C18H38 n-alkane material, *Experimental Thermal and Fluid Science* (2019), doi: https://doi.org/10.1016/j.expthermflusci.2019.109854

SNS OPTICAL FIBER SENSOR FOR DIRECT DETECTION OF PHASE TRANSITIONS IN C18H38 N-ALKANE MATERIAL

Wei Han[1], Marek Rebow[2], Xiaokang Lian[1], Dejun Liu[1], Gerald Farrell[1], Qiang Wu[3], Youqiao Ma[4] and Yuliya Semenova[1]

[1]Photonics Research Centre, Technological University Dublin, Kevin Street, Dublin 8, Ireland

[2]College of Engineering and Built Environment, Technological University Dublin, Bolton Street, Dublin 1, Ireland

[3]Department of Mathematics, Physics and Electrical Engineering, Northumbria University, Newcastle Upon Tyne, NE1 8ST, United Kingdom

[4]Depatment of Electrical and Computer Engineering, Dalhousie University, Halifax, Canada

Key words: Optical fiber sensor, Phase change materials (PCMs), n-octadecane

Abstract

A single-mode-no-core-single-mode (SNS) fiber optical sensor for the detection of solid-liquid and liquid-solid phase changes in C18H38 n-alkane (n-octadecane) is proposed and demonstrated. The transmission-type sensor probe consists of a short section of no-core fiber sandwiched between two sections of a single-mode fiber. Phase changes in n-octadecane are accompanied by large step-like variations of its refractive index (RI). Such a large discontinuous change of the n-octadecane's RI during its phase transition leads to the corresponding step-like change in the transmitted optical power that can reliably indicate the phase change of the sample in the vicinity of the sensor. The proposed sensor probe is simple, accurate and is capable of detecting the material's phase based on a single measurement. The results of this work suggest that the proposed sensor is potentially capable of detecting liquid-solid phase changes in other materials whose thermo-optic properties are similar to those of n-octadecane.

Introduction

Phase change materials (PCMs) are widely used in thermal energy storage applications due to their ability to absorb, store and release large amounts of energy during melting or solidification. To achieve higher efficiency in energy storage applications, it is necessary to be able to accurately detect the phase changes in PCMs. A typical indirect approach to the detection of phase changes in a PCM involves monitoring of the material temperature with standard electrical sensors, such as thermocouples. However this approach has some limitations. For example, due to its high thermal conductivity, a thermocouple can transfer the heat to or from the sample, which in turn may affect the phase state in its vicinity and thus cause errors in the phase change detection [1].

Therefore in practice, direct detection of the phase changes in PCM is preferred. For optically transparent materials, direct observation of the solid-liquid interface is possible [2]. However this method is not suitable for opaque materials. Both X-ray tomography and radiography allow for the visualization of solid-liquid interfaces regardless of optical transparency [3-5] and thus both methods can detect changes in the material density associated with phase changes, however these methods are laboratory-based and incapable of providing real time

information. During melting or solidification, most PCMs show changes in electrical resistance, therefore resistance diagnostics has also been used for the detection of phase changes [6]. However this method is only applicable to bulk material samples and does not allow for phase detection at a specific points within the sample's volume. Differential scanning calorimetry (DSC) can be applied to characterize PCMs, and it also can be used to detect the phase states [7]. However, it is also incapable of detection the phase state at a specific point within the sample's volume, making it unsuitable for energy storage applications which involve large PCM volumes.

Fiber optic sensors offer the advantages of a simple structure, high sensitivity, low cost, and immunity to electromagnetic interference making them popular candidates for measurements of many physical parameters, including temperature [8-9] and strain [10-11]. Several studies considered applications of fiber optic sensors in detection of phase changes. For example, Arnon *et al.* [12] developed a fiber-optic evanescent wave spectroscopic method for detection of solid-liquid phase changes in water based on the changes of the sample's absorbance. However the technique is relatively complex and requires the use of special silver halide based fibers. Rahul *et al.* [13] demonstrated detection of phase states in a paraffin wax using a single-mode-multimode reflective fiber probe. The operating principle of their proposed senor relied on the detection of strain acting upon the fiber probe due to its micro-bending in the solid phase. Mani *et al.* [14] reported a Fresnel reflection fiber sensor for monitoring the crystallization of water and aqueous solution of NaCl based on changes of reflectivity of the fiber probe associated with changes in the material RI during the phase transition. Similar Fresnel reflection fiber probe was reported recently for C18H38 n-alkane (n-octadecane) [15]. Although this method is simple and accurate, it requires multiple measurements to realize continuous optical power monitoring since it relates the phase change to a relative change in the optical power reflected by the probe's end immersed in the material sample. Moreover, such Fresnel sensors are highly susceptible to disturbances within the material, including fluctuations in reflections due to air bubbles or impurities, making it less reliable in real world applications.

In this paper we propose and experimentally demonstrate a novel fiber optic sensor for the in-situ detection of solid-liquid and liquid-solid phase transitions in n-octadecane. The sensor probe is fabricated by splicing a section of no-core fiber between two standard SMFs. The phase change is detected by monitoring the normalized optical power transmitted through the sensor probe immersed into the sample. N-octadecane, whose physical properties make it attractive for a number of applications, such as thermal control in a spacecraft [16], or in comfort clothing, to maintain the appropriate temperature close to that of human skin [17]. In this work n-octadecane was chosen for the proof of principle demonstration of the proposed sensing method because the material's crystallization occurs over a narrow range of temperatures, with a high degree of repeatability. In addition, the closeness of the solidification point to room temperature allows for a simpler experimental set up. Moreover, the material is transparent in the liquid phase and opaque in the solid phase with a small mushy zone, which makes it possible to observe the phase change in the vicinity of the probe as the means of validation.

The sensor proposed in this work allows for a simple, low cost, accurate and reliable in-situ detection of liquid-solid and solid-liquid phase changes in n-octadecane without the need for temperature measurements. Compared to the previously reported Fresnel reflection sensor [15], the sensor proposed here offers the capability of detection of a specific phase state based on a single measurement. Moreover, the binary nature of the sensor's output (namely, "low" or "high" power states) allows to eliminate small fluctuations due to strain and thermal

convection, making the proposed sensor resistant to various disturbances in practical applications.

Experimental setup and operating principle

The proposed sensor probe and its characterization setup are shown in Figure 1. The system consists of a laser (NETTEST, central wavelength 1550 nm), a 3 dB coupler, fiber sensor probe and a dual-channel optical power meter (4100, Dbm Optics). The 3 dB coupler splits input power from the laser source between Channel 1 of the optical power meter serving as a reference and the fiber sensor probe. The fiber probe output is connected to Channel 2 of the optical power meter in a ratiometric scheme [15]. The sensor probe is fabricated from a short section of no-core fiber (Thorlabs, FG125LA) sandwiched between two sections of a standard single-mode fiber (Thorlabs, 1550BHP) by fusion splicing. The coating is stripped from the no-core fiber section and the single-mode fiber near the no-core section is marked with blue ink to allow for better visibility of the probe's position when it is immersed in the n-octadecane sample. Since the liquid phase sample is transparent while the solid phase sample is not, visual observation of the blue mark indicates that the material is in its liquid phase at the location of the mark. The temperature in the vicinity of the fiber sensor probe is monitored with a K-type thermocouple placed in close proximity (~2 mm) to the fiber probe and at the same distance from the heat source as the fiber probe. The thermocouple has an error of $0.004 \times T$, where T is the actual temperature. A Peltier element is used as a thermoelectric heater/cooler.

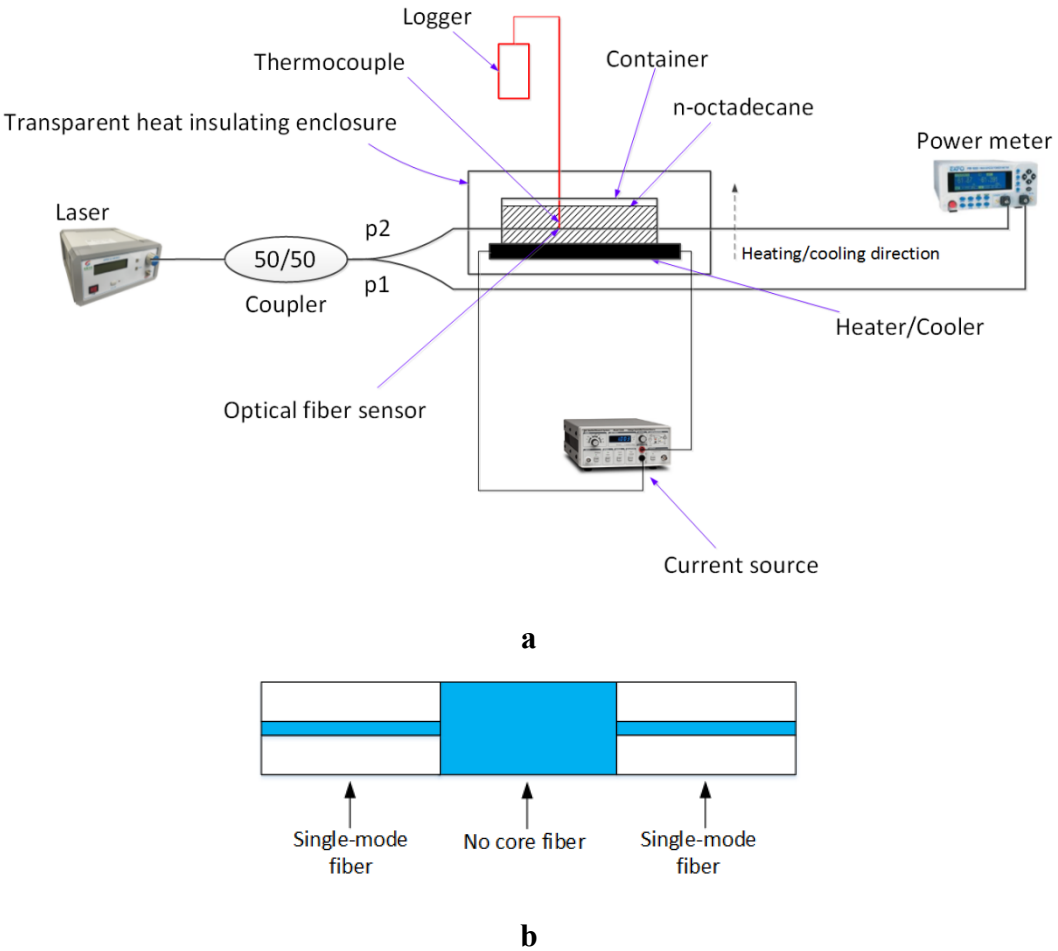

Fig. 1. (a) Schematic diagram of the experimental setup; (b) fiber probe schematic.

Assuming the input and output single-mode fibers are the same and the length of the no-core fibre section is L, when the sensor is immersed in the solid sample whose RI is higher than that of the no-core fiber, the field in the no-core fiber consists of leaky modes and the output of the sensor can be described as [18]:

$$\mathrm{P} = 10log_{10}\left(\frac{\left|\int_0^\infty E(L)E_0 ds\right|^2}{\int_0^\infty |E(L)|^2 ds \int_0^\infty |E_0|^2 ds}\right) \quad (1)$$

where $E(L)$ is the electrical field at the end of no-core fiber, E_0 is the electrical field of the fundamental mode of the single-mode fiber. The electrical field of the leaky mode in the no-core fiber can be described as [18]:

$$E(L) = \sum_{m=1}^{M} b_m E_m e^{i\beta_m L} e^{-a_m L} \quad (2)$$

where E_m and b_m are electrical field and excitation coefficients of the mth leaky mode in the no-core fiber respectively, β_m and a_m are the propagation constant and attenuation constants respectively and M is the total number of modes in the no-core fiber.

When the sensor is immersed in the liquid sample whose RI is lower than that of the no-core fiber, the field of the no-core fiber consists of guided modes which can be described as [19]:

$$E(L) = \sum_{m=1}^{M} b'_m E'_m e^{j\beta'_m L} \quad (3)$$

where b'_m is the excitation coefficient of each mode, E'_m are the eigenmodes of the no-core fiber and β'_m are the propagation constants of each eigenmode of the no-core fiber.

From [20], the RI values for n-octadecane are known to be approximately 1.468 for the solid and 1.432 for the liquid phase at a wavelength of 600 nm. We have used the data in [20] and the Cauchy's equation [21] to calculate the approximate values of the refractive index of the n-octadecane in the wavelength range of interest for our experiment. The results of the calculations showed that the RI of n-octadecane at a wavelength of 1550 nm decreases only by about 0.08% for the solid and by 0.07% for the liquid phase compared to the values at 600 nm. The RI of n-octadecane decreases with temperature, but it should be noted that while in the solid phase RI experiences only a small decrease with the increase in temperature, as soon as n-octadecane becomes liquid, its RI decreases sharply from circa 1.468 to 1.432 [20]. The RI of the no-core silica fiber is 1.444 at 1550 nm. When the sensor is immersed in the solid n-octadecane, since the RI of the material sample is higher than that of the no-core fiber, light propagating through the no-core section is no longer confined to the fiber due to the absence of total reflection, which results in a low power output from the sensor. As soon as the n-octadecane melts into liquid, the RI of the sample decreases to 1.4226, becoming lower than the RI of the no-core fiber. The modes with the incident angles larger than the critical angle will be totally reflected so that the output power increases sharply. Therefore the phase state of n-octadecane in the vicinity of the fiber probe can be detected by a single measurement of the transmitted power, and the phase change can thus be determined by detecting the step-like change in the sensor's output.

Figure 2 illustrates the simulated optical power distributions within the no-core fiber section (left) and the transmitted output powers (right) for the sensor immersed in solid (a) and liquid (b) n-octadecane. Z axis indicates the direction of light propagation. The monitor value shown on the right-side graphs represents the intensity of light along the Z axis. The

simulations have been carried out using commercial software package BeamPROP (Rsoft, Pasadena, CA, USA). In the simulations the free space wavelength was set as 1550 nm, the RIs of the single-mode fiber core and cladding were set as 1.4504 and 1.4447 respectively, and the RI of the no-core fiber was set as 1.444. The lengths of the two sections of the single-mode fiber spliced with the no-core fiber were set equal to 1 mm and the length of the no-core fiber was 5 mm, similar to those in the experiment. The diameters of the core and cladding of the single-mode fiber were assumed 8.3 µm and 125 µm respectively and the diameter of the no-core fiber was 125 µm. In the simulations the RI of the solid n-octadecane was assumed equal to 1.468 and that of the liquid n-octadecane RI was set to 1.432. From the simulations it can be seen, that when the material sample is solid (Fig. 2a), the light power launched from the input single-mode fiber section into the no-core fiber (Z=100 µm) leaks out of the no-core fiber into the solid sample whose RI is higher than that of the no-core fiber, causing low power output. As soon as the sample melts into a liquid (Fig. 2b), the RI of the material sample becomes smaller than that of the no core fiber, so that the input optical power is strongly confined within the no-core fiber section leading to a higher power coupled into the output single-mode fiber and thus leading to the higher output of the sensor.

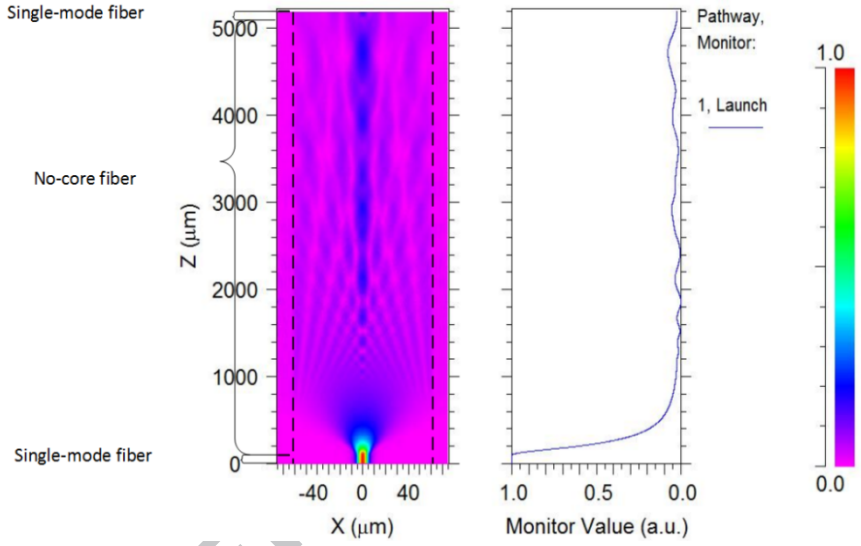

a

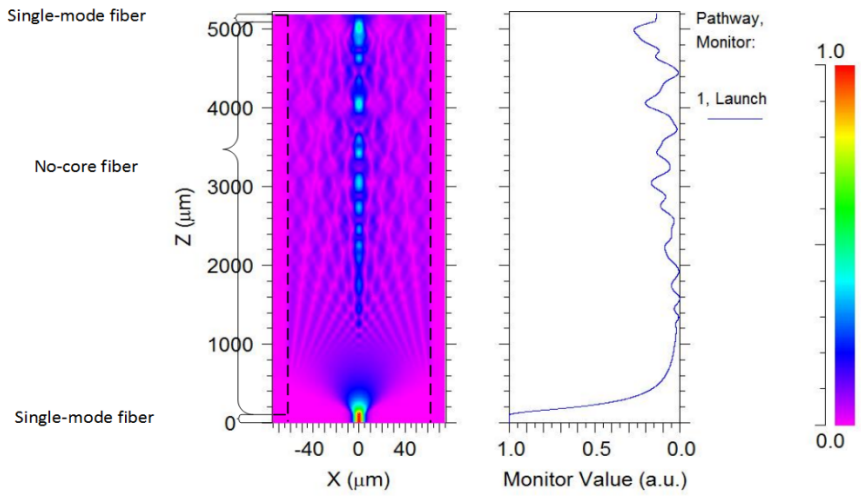

b

Fig.2 Simulated output power distributions (left) and intensity of the light along the Z axis (right) when the sensor is immersed in: (a) solid, (b) liquid sample.

Experimental results and discussion

As a preliminary step, the sensor was initially characterized in air (prior to immersing it in n-octadecane. Fig. 3 illustrates the measured normalized output spectrum of the fiber probe. From the figure it can be seen that the output power varies with the source wavelength, but the maximum power variation is less than 4.5 dB over a wide wavelength range from 1520 nm to 1600 nm. In our experiments the laser wavelength was set at 1550 nm.

In order to experimentally demonstrate the operation of the proposed sensor, a series of heating and cooling experiments were carried out for a 25 ml sample of n-octadecane with 99 % purity (Sigma Aldrich), using the experimental setup shown in Figure 1. The fiber probe and the thermocouple were immersed in the n-ocatdecane sample and the thermocouple was fixed in the vicinity of the fiber probe (~2 mm). The thermocouple was connected to a logger to record the temperature of material close to the fiber probe. To ensure the stability of the surrounding temperature, the experimental setup was placed inside a transparent heat insulating enclosure. A digital camera was also placed inside the insulating enclosure and connected to a laptop PC for recording images. The camera shutter was also controlled by the PC. The photo images were taken at the same time as the output power of the sensor and temperature data were recorded with steps of 0.5 °C.

At the start of the heating experiment the temperature of the Peltier was set to 20°C, well below the temperature range of interest near the phase change point (circa 27.5°C). Then both the sample and the Peltier were kept inside the transparent insulating enclosure for a sufficient period of time to ensure the starting temperature of 20 °C. This ensured that the temperature of the surrounding environment did not inadvertently cause sporadic phase changes in the sample and thus the only heat source that could cause a phase change was the Peltier heater. This resulted in a well-defined interface between the solid and liquid n-octadecane that was easily observable by the camera. The Peltier heater was then set to the temperature of 50 °C and began pumping heat into the material sample from the bottom of the cuvette upwards, causing a slow progressive melting of n-octadecane, so that a visible interface between the solid and liquid phases could be seen moving up through the sample and recorded by the camera.

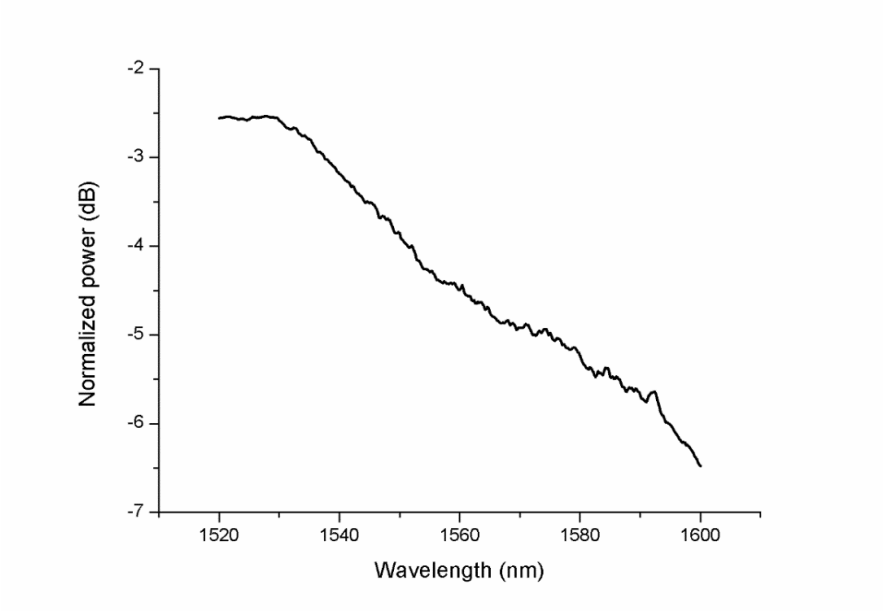

Fig.3 Measured transmission spectrum of the sensor

Prior to the cooling experiment, in order to ensure a well-defined sharp interface between the solid and liquid n-octadecane, the temperature of the heater was first set to 30 °C for a period of time sufficient for the sample's overall temperature to reach 30 °C. Then the Peltier heater's current direction was reversed so that the cold side of the heater, set at the temperature of 15 °C, was in contact with the sample, causing its slow solidification up from the bottom of the cuvette and producing a sharp and clearly visible interface between the liquid and solid phases that was recorded by the camera.

Based on the data returned by the fiber optic sensor and the thermocouple, Fig. 4 illustrates the dependence of the normalized output power of the sensor probe versus the temperature of n-octadecane. Every data point in Fig. 4 is an average of five different heating/cooling experiments.

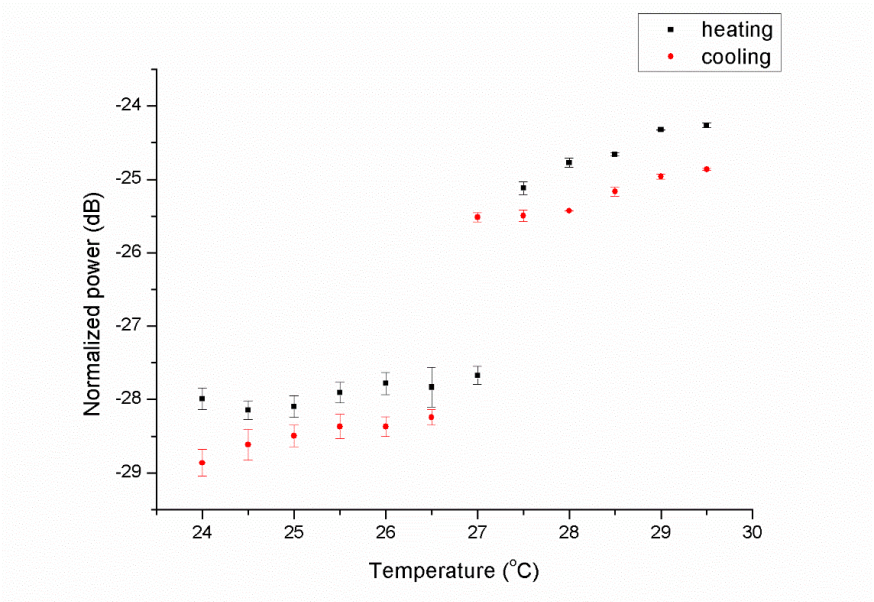

Fig.4 The response curve of the experiments

As can be seen from Fig. 4, in the range of temperatures from 24 °C to 27 °C during heating the normalized transmitted power remains relatively low averaging near -28 dB. As soon as the temperature of the material reaches ~27.5 ºC the sample melts into a liquid and the output power increases sharply to about -25 dB, which is in agreement with the simulation results. In the liquid phase light rays with an incident angle larger than the critical angle experience total internal reflection, which causes a sudden increase in the transmitted power. The critical angle can be described as [21]

$$\theta_c = arcsin\frac{n_2}{n_1} \tag{5}$$

where n_2 and n_1 are the RIs of the material and fiber respectively.

It can also be seen that the output power level continues to increase in the liquid phase with temperature as a result of the decrease of the liquid sample's RI. As the liquid sample is heated from 27.5°C to 29.5°C, the probe's output power increases slightly by about 0.7 dB, which is consistent with a temperature-induced decrease of the material's RI in the liquid phase.

The average error of the data in the solid phase is 0.16 dB, while that in the liquid phase is 0.04 dB. One possible reason for such a difference in errors is likely the sensitivity of the fiber probe to strain and bending. The strain and stress forces acting upon the fiber sensor in the solid phase are greater in comparison with those in the liquid phase as a result of the higher material density of solid n-octadecane [22. 23]. Moreover, restricted mobility of the fiber probe in the solid phase may result in random micro-bending of the fiber leading to the variations in the power output.

It can also be observed that the average power levels in solid and liquid phases are also slightly different for the cooling and heating cycles. This also could be attributed to the influence of stain and bending forces on the probe. Since in each of the experiments the directions of movement of the solid phase front were different, this led to the difference in bending forces and resulting curvature of the probe.

The recorded images show that the sensor output step change aligns very well with the visual observations. Figure 5 shows a series of images of the n-octadecane sample taken at different temperatures during the heating experiment. From the photos it can be seen that at 27 °C the sensor is not visible, which means the sample surrounding the sensor is solid, while at 27.5 °C the fiber sensor is visible, which proves that above 27.5 °C the sample surrounding the sensor is in liquid phase.

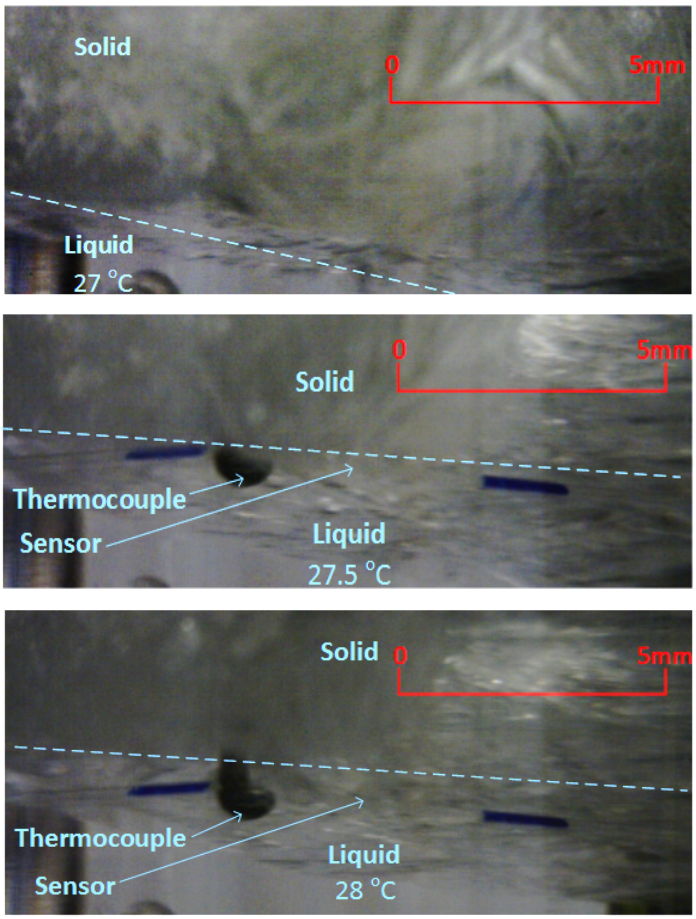

Fig.5 Photographs of the sample at different temperatures during heating experiment

On cooling, as the temperature decreases to 26.5 °C the n-octadecane sample solidifies. The output power decreases immediately from -25.5 dB to -28.2 dB as there is no total reflection for the light rays in the no-core fiber section. Figure 6 illustrates images of the n-octadecane sample taken at different temperatures during cooling. From the photos it can be seen that at 27.5 °C and 27 °C the sensor is visible, which means the sample surrounding the sensor is liquid, while at 26.5 °C the fiber sensor is no longer visible, which proves that from 26.5 °C the sample phase surrounding the sensor is solid.

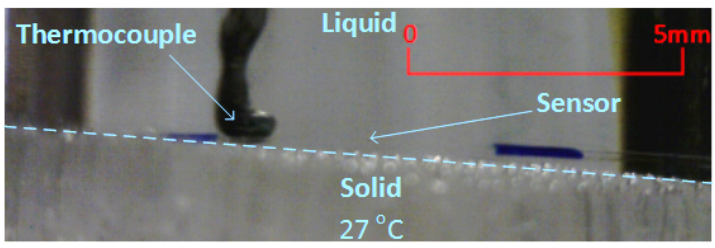

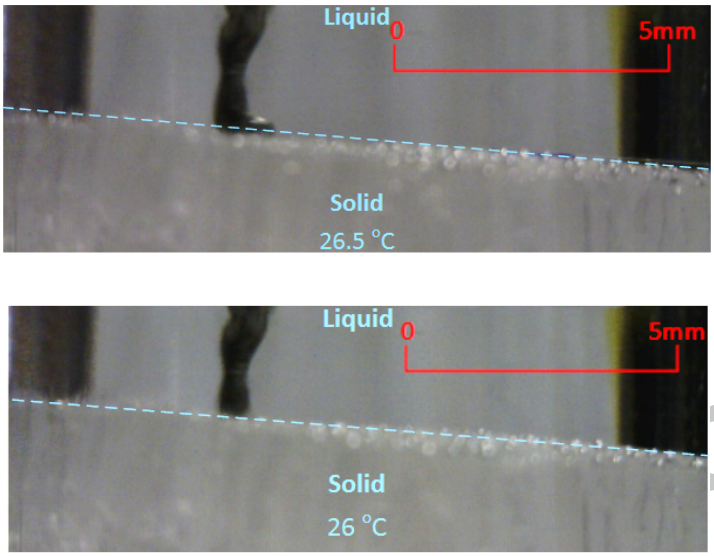

Fig.6 Photographs of the phase change front at different temperatures during cooling.

Based on the experimental data above, melting and crystallisation temperatures for n-octadecane are 27.5°C and 26.5 °C, which is in a good agreement with those reported in [22].

From the above experiments it can be seen that due to the sudden change of the RI of the sample associated with solid-liquid or liquid-solid phase transitions, the output power level from the sensor probe can be used as a measure or an indicator of the material's phase: the output power is low when the sensor is immersed into a solid n-octadecane and if the sensor is immersed into a liquid n-octadecane, the output power is high. Therefore the specific phase can be detected by a single measurement, which is an improvement compared to the sensor we proposed previously, since that sensor needs at least two distinct measurements to detect the phase of the sample [15].

Signal processing can be used to improve the reliability of detection of the phase change. The first step in signal processing is to digitize the outputs from the fiber sensor and the reference fiber following optoelectronic conversion. Subsequently software based averaging and noise reduction using low pass filtering or more sophisticated signal processing can be carried out to improve the signal-to-noise ratio. Finally the sensor output power level is compared to a reference power level chosen as an intermediate power equidistant from the lowest and highest possible outputs from the sensor, recorded during the heating/cooling cycles. The result from the comparison will indicate whether the material is in solid or liquid phases at the location of the probe.

To study of the sensor's ability to operate in non-laboratory conditions where temperature and thermal convection changes are less controlled and less predictable, another cooling experiment was carried out, during which the temperature inside the enclosure was set to 15 °C and liquid n-octadecane was left to cool naturally. The initial temperature of the n-octadecane was 30 °C. Unlike cooling from the bottom of the container in the former experiment, in this case cooling of the sample occurs from its outer walls towards the center of the sample, so that the increasing pressure (due to the increasing sample density) is applied to the fiber from all directions. In such conditions there is no visible solid-liquid interface and the phase change is likely to be affected by various random factors. This in turn may result in

larger fluctuations of the sensor output. The purpose of this experiment was to evaluate the performance of the sensor in such conditions, and its results are illustrated in Fig. 7, where each point is an average of five measurements. As it can be seen from the figure, in the temperature range from 24 °C to 26.5 °C, the power changes from -28.8 dB to -28.5 dB, which means that the sensor's output is low and the n-octadecane is in its solid state in the vicinity of the sensor. In the temperature range from 27 °C to 29 °C the output power changes from -25.2 dB to -24.6 dB. The output power is high indicating that the sensor is immersed in liquid n-octadecane.

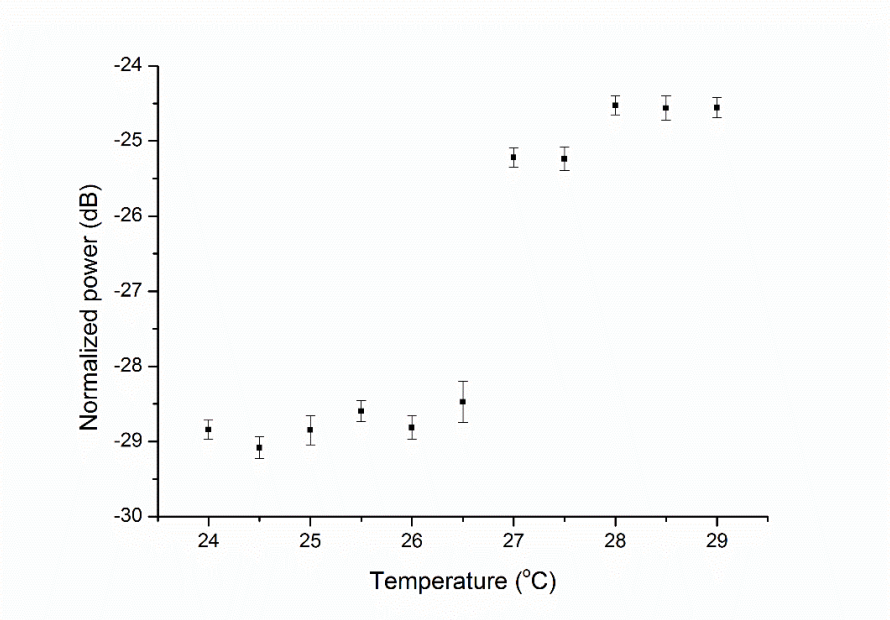

Fig.7 The result of the cooling naturally experiment.

The average error of the whole experiment result is 0.16 dB, which is larger than in the previous experiment (Fig.4). This is likely due to that in the latter experiment, the changes in the values and direction of bending and strain forces acting upon the fiber immersed in the sample were random during the whole process. However, even though the bending and the strain change randomly, it can be seen from Fig.7 that the information provided by the sensor allows for the unambiguous detection of the occurrence of solidification at 26.5 °C, which is exactly the same result as in the former experiment. It is can be concluded thus that the sensor is capable of providing reliable phase information even when it operates in a more realistic non-laboratory environments where solidification or melting is not unidirectional. In this is also demonstrates a better ability to deal with real-world conditions than the sensor we proposed previously [15].

Conclusion

A novel optical fiber sensor based on an SNS fiber structure for detection of the phase state of n-octadecane has been proposed and demonstrated experimentally. From the experimental results it can be seen that the sample becomes liquid at approximately 27.5 °C and solidification occurs at 26.5 °C, which is very close to the values reported in literature [22]. Since the output power level of the sensor changes abruptly from low to high with the transition of n-octadecane from solid to liquid phase (and vice versa), detection of the specific phase of the n-octadecane can be realized with a single power measurement and

without the knowledge of the sample's temperature. The sensor's performance is resistant to external perturbations, such as occurrence of air bubbles, impurities and mechanical disturbances. It can be easily integrated with a control unit for practical energy storage systems. The results of this work suggest that the proposed sensor is potentially capable of detecting liquid-solid and solid-liquid phase changes in other materials whose thermo-optic properties are similar to those of n-octadecane, namely in the materials whose phase transitions are accompanied by a step change of refractive index between the values lower and higher than that of the silica fiber at the operating wavelength of the optical source.

References

1. Anderson, R. L., Adams, R. K., & Duggins, B. C. (1979). Limitations of thermocouples in temperature measurements (No. CONF-790505-14). Oak Ridge National Lab., TN (USA).

2. Akamatsu, S., Faivre, G., & Ihle, T. (1995). Symmetry-broken double fingers and seaweed patterns in thin-film directional solidification of a nonfaceted cubic crystal. *Physical Review E*, *51*(5), 4751.

3. Shuaia, S., Guo, E., Phillion, A.B., Callaghan, M.D., Jing, T., Lee, P.D. (2016), Fast synchrotron X-ray tomographic quantification of dendrite evolution during the solidification of MgSn alloys. Acta Materialia, 118, 260-269

4. Murphy, A. G., Browne, D. J., Mirihanage, W. U., & Mathiesen, R. H. (2013). Combined in situ X-ray radiographic observations and post-solidification metallographic characterisation of eutectic transformations in Al–Cu alloy systems. *Acta Materialia*, *61*(12), 4559-4571.

5. Nguyen-Thi, H., Reinhart, G., Jaoude, G. S. A., Mathiesen, R. H., Zimmermann, G., Houltz, Y., & Murphy, A. G. (2013). XRMON-GF: A novel facility for solidification of metallic alloys with in situ and time-resolved X-ray radiographic characterization in microgravity conditions. *Journal of Crystal Growth*, *374*, 23-30.

6. Salvi, C., & Garandet, J. P. (2001). A novel resistance measurement technique in the field of directional solidification. *Review of Scientific Instruments*, *72*(1), 255-262.

7. Lazaro, A., Peñalosa, C., Solé, A., Diarce, G., Haussmann, T., Fois, M., & Cabeza, L. F. (2013). Intercomparative tests on phase change materials characterisation with differential scanning calorimeter. *Applied Energy*, *109*, 415-420.

8. Ju, Y., Ning, S., Sun, H., Mo, J., Yang, C., Feng, G., & Zhou, S. (2018). Temperature and refractive index measurement based on a coating-enhanced dual-microspheric fiber sensor. *Laser Physics*, *28*(7), 076203.

9. Tan, J., Feng, G., Zhang, S., Liang, J., Li, W., & Luo, Y. (2018). Dual spherical single-mode-multimode-single-mode optical fiber temperature sensor based on a Mach–Zehnder interferometer. *Laser Physics*, *28*(7), 075102.

10. Tian, J., Jiao, Y., Fu, Q., Ji, S., Li, Z., Quan, M., & Yao, Y. (2018). A Fabry–Perot interferometer strain sensor based on concave-core photonic crystal fiber. *Journal of Lightwave Technology*, *36*(10), 1952-1958.

11. Liu, Y., Blokland, W., Long, C. D., Riemer, B. W., Wendel, M. W., & Winder, D. E. (2018). Strain measurement in the spallation target using high-radiation-tolerant fiber sensors. *IEEE Sensors Journal*, *18*(9), 3645-3653.

12. Millo, A., Raichlin, Y., & Katzir, A. (2005). Mid-infrared fiber-optic attenuated total reflection spectroscopy of the solid–liquid phase transition of water. *Applied Spectroscopy*, 59(4), 460-466.

13. Kumar, R., Han, W., Liu, D., Ng, W. P., Binns, R., Busawon, K., & Yuan, J. Yu, C., Shu, H., Li, X.A., Guo, T., Farrell, G., Semenova, Y., Wu, Q. (2018). Optical fibre sensors for monitoring phase transitions in phase changing materials. *Smart Materials and Structures*, 27(10), 105021.

14. Mani, P., Rallapalli, A., Machavaram, V. R., & Sivaramakrishna, A. (2016). Monitoring phase changes in supercooled aqueous solutions using an optical fiber Fresnel reflection sensor. *Optics Express,* 24(5), 5395-5410.

15. Han, W., Rebow, M., Liu, D., Farrell, G., Semenova, Y., & Wu, Q. (2018). Optical fiber Fresnel reflection sensor for direct detection of the solid-liquid phase change in n-octadecane. *Measurement Science and Technology*, 29(12), 125107.

16. Trevino, L. A., & Orndoff, E. S. (2000). Advanced space suit insulation feasibility study (No. 2000-01-2479). SAE Technical Paper.

17. Mondal, S. (2008). Phase change materials for smart textiles–An overview. *Applied Thermal Engineering*, 28(11-12), 1536-1550.

18. Yang, L., Xue, L., Che, D., & Qian, J. (2012). Guided-mode-leaky-mode-guided-mode fiber structure and its application to high refractive index sensing. *Optics Letters*, *37*(4), 587-589.

19. Wu, Q., Semenova, Y., Wang, P., & Farrell, G. (2011). High sensitivity SMS fiber structure based refractometer–analysis and experiment. *Optics Express*, *19*(9), 7937-7944.

20. Kim, M. S., Kim, M. K., Jo, S. E., Joo, C., & Kim, Y. J. (2016). Refraction-Assisted Solar Thermoelectric Generator based on Phase-Change Lens. *Scientific Reports*, *6*, 27913.

21. Jenkins, F. A., & White, H. E. (1937). *Fundamentals of Optics*. Tata McGraw-Hill Education.

22. Vélez, C., Khayet, M., & De Zárate, J. O. (2015). Temperature-dependent thermal properties of solid/liquid phase change even-numbered n-alkanes: n-Hexadecane, n-octadecane and n-eicosane. *Applied Energy 143*, 383-394.

23. Wolfram/Alpha Knowledgebase www.wolframalpha.com/input/?i=chemical%2BN-octadecane.

We declare that we have no financial and personal relationships with other people or organizations that can inappropriately influence our work, there is no professional or other personal interest of any nature or kind in any product, service and/or company that could be construed as influencing the position presented in, or the review of, the manuscript entitled, “SNS optical fiber structure sensor for direct detection of the phase transition in c18h38 n-alkane material”

1. An all optical fiber sensor based on a singlemode-no-core-singlemode (SNS) fiber structure for detecting the solid-liquid phase change in a phase change material (n-octadecane) is proposed and experimentally demonstrated.
2. The sensor relies on the step change of the output power caused by the change of the n-octadecane's refractive index during the phase change, allowing for direct detection of the phase through one simple measurement.
3. The sensor has strong resistance to disturbances since the output signal is always low for the solid and high for the liquid state.
4. The sensor is capable of detecting the supercooling of the material sample.